*Research Paper*
*Computational Methods for Differential Equations*
http://cmde.tabrizu.ac.ir
Vol. 10, No. 1, 2022, pp. 225-235
DOI:10.22034/cmde.2020.41858.1812

# An anomalous diffusion approach for speckle noise reduction in medical ultrasound images

**Maryam Sadat Seidzadeh, Hadi Roohani Ghehsareh*, and Seyed Kamal Etesami**
Department of Mathematics, Faculty of Applied Sciences, Malek Ashtar University of Technology, Shahin Shahr, Iran.

**Abstract**

Medical ultrasound images are usually degraded by a specific type of noise, called "speckle". The presence of speckle noise in medical ultrasound images will reduce the image quality and affect the effective information, which can potentially cause a misdiagnosis. Therefore, medical image enhancement processing has been extensively studied and several denoising approaches have been introduced and developed. In the current work, a robust fractional partial differential equation (FPDE) model based on the anomalous diffusion theory is proposed and used for medical ultrasound image enhancement. An efficient computational approach based on a combination of a time integration scheme and localized meshless method in a domain decomposition framework is performed to deal with the model. In order to evaluate the performance of the proposed de-speckling approach, it is used for speckle noise reduction of a synthetic ultrasound image degraded by different levels of speckle noise. The results indicate the superiority of the proposed approach in comparison with classical anisotropic diffusion denoising model (Catté's pde model).

**Keywords.** Medical ultrasound images, Images denoising, Fractional Perona-Malik equation, Localized meshfree method, Domain decomposition method.

**2010 Mathematics Subject Classification.** 68U10, 65D12, 35R11.

## 1. Introduction

Ultrasonography is recognized as one of the most powerful techniques for imaging fine organs and tissues in clinical diagnosis and therapeutic approaches. However, ultrasound images are often damaged by speckle noise during image acquisition, which can complicate the correct diagnosis of lesions with low-intensity [20, 61]. Therefore, detecting the speckle noise in the images and performing techniques to despeckle the corrupted images are important issues in medical image analysis and diagnosis [38]. Several approaches have been proposed and developed for speckle reduction and improving the quality of medical images for better human interpretation. Using despeckle filters is one of the easiest, yet most common speckle noise reduction approach which have been widely applied to enhance medical images. These filters are performed on spatial or frequency domain of an image. Some of the filters introduced in the spatial domains are, noise filtering algorithms based on the local statistics of the image [35], median filter [40, 46], speckle reducing anisotropic diffusion filter [21, 66], total-variation (TV) minimization algorithm [60], combination of diffusion and total variation models [41], etc. Also, there are various approaches based on transform domain for speckle noise reduction in medical images. Some denoising approaches based on the wavelet transformation have been introduced and used to enhance medical ultrasound images [10, 23, 42]. Abazari and Lakestani have formulated a fourier based discrete shearlet transform [1] and also a hybrid denoising algorithm based on combining of the shearlet transform method with the Yaroslavsky's filter [2] to reduce the noises of ultrasound medical images. Recently, a novel speckle noise removal approach based on the combination of a log-transform method and a non-subsampled shearlet transform technique has been successfully introduced by Abazari and Lakestani [3]. Partial Differential Equations (PDE)- based image denoising approaches, are one of the important class of image enhancement and restoration techniques which have been attracted attention and successfully used during the recent years (see [7] and references therein). One of

Received: 17 September 2020 ; Accepted: 25 December 2020.
∗ Corresponding author. Email: hadiroohani61@gmail.com.

the most fundamental PDE-based models in the field of image processing is the Perona-Malik (PM) equation which has been proposed in 1990 [43]. The Perona-Malik model is a special case of anisotropic diffusion equations, which the rate of diffusion is controlled by an edge stopping function depending on the local image gradient. The Perona-Malik model is defined as follows:

$$\begin{cases} \frac{\partial u(\mathbf{x},t)}{\partial t} = \nabla \cdot \big[g(\mid \nabla u(\mathbf{x},t) \mid)\nabla u(\mathbf{x},t)\big], \quad (\mathbf{x},t) \text{ in } \Omega \times \mathrm{I}, \\ \frac{\partial u(\mathbf{x},t)}{\partial n} = 0, \quad \text{on } \mathrm{I} \times \partial\Omega, \\ u(\mathbf{x},0) = u_0(\mathbf{x}), \text{ in } \Omega. \end{cases} \tag{1.1}$$

Where $\Omega$ is typically a rectangular shaped bounded domain in $\mathbb{R}^2$ which denotes the entire image region, $\frac{\partial u}{\partial n}$ is the outward unit normal to the image boundary, $\partial\Omega$, $\mathrm{I} = [0,T]$ is a scaling time interval, $g(.)$ is a smooth non-increasing function, $g(s) \geq 0$, $g(0) = 1$ and $g(s) \longrightarrow 0$ as $s \longrightarrow \infty$. The behaviour of solutions of the Perona-Malik problem have been investigated in several literature [9, 27, 34, 44]. Unfortunately, it has been shown that the classical Perona-Malik equation behaves locally like backward diffusion process which is an ill-posed evolution problem [9, 34, 63]. To overcome this drawback, Catté et al. introduced a development approach to regularize the nonlinearity term in the equation (1.1) [9]. They proposed replacing the diffusivity $g(\mid \nabla u \mid)$ of the Perona-Malik model by a little change $g(\mid \nabla u_\sigma \mid)$ with $u_\sigma = G_\sigma * u$, where $G_\sigma$ is a smooth kernel Gaussian of variance $\sigma$. According to their suggestion, the governing equation in (1.1) is considered as follows [6, 9]:

$$u_t - \nabla \cdot (g(\mid \nabla G_\sigma * u \mid)\nabla u) = f(u^0 - u), \text{ in } \Omega \times \mathrm{I}, \tag{1.2}$$

where $f(.)$ is a Lipschitz continuous, nondecreasing function, $f(0) = 0$, and $u_0 \in L_\infty(\Omega)$.
The typical choices of diffusivities are:

$$g(s) = \frac{1}{1 + (s/k)^2}, \text{ and } g(s) = \exp(-(s/k)^2). \tag{1.3}$$

Here $k$ is a given threshold that controls the pixels that should be preserved or enhanced during the diffusion process [62].
In recent decades fractional calculus has attracted the great attention as an expansion of the classical calculus [59] and widely used to describe many complex systems [11, 15, 24–26, 39, 45]. Recently, theory of fractional calculus is widely developed and successfully applied to many image processing applications such as image enhancement, image denoising, image edge detection, image segmentation, image registration, image recognition, image compression and etc [65].
Compared with integer-order partial differential equation filters for image denoising, the fractional ones have better performances to satisfy the requirements of a proper image enhancement [65]. Due to high capability and potential of fractional calculus for image enhancement, several image denoising algorithms based on it, have been proposed in recent years. Bai and Feng [8] have proposed an anisotropic diffusion model with space-fractional derivatives for image denoising. Zhang et al. [67, 68] generalized the TV model based on the Grünwald-Letnikov fractional derivative and proposed an efficient TV filter for enhancing digital images. A fully fractional anisotropic diffusion with spatial and time fractional derivatives has been introduced and performed for noise removal [28]. Thier results show that the model can preserve edges more efficiently than the classical diffusion models. In order to achieve the optimal balance between performance of the diffusion model and the preservation of image feature in ultrasound medical image despeckling process, in this manuscript an anomalous sub-diffusion model with time-fractional derivative in sense of Caputo's definition has been proposed as follows:

$$\begin{cases} {}_0^c D_t^\alpha u(\mathbf{x},t) = \nabla \cdot (g(\mid \nabla G_\sigma * u \mid)\nabla u), \text{ in } \Omega \times \mathrm{I}, \\ \frac{\partial u}{\partial n} = 0, \text{ on } \mathrm{I} \times \partial\Omega, \\ u(\mathbf{x},0) = u_0(\mathbf{x}), \text{ in } \Omega, \end{cases} \tag{1.4}$$

where ${}_0^c D_t^\alpha u$ denotes the Caputo fractional derivative of order $\alpha$,

$${}_0^c D_t^\alpha u(\mathbf{x},t) = \frac{1}{\Gamma(1-\alpha)} \int_0^t \frac{\partial u(\mathbf{x},\tau)}{\partial \tau} \frac{d\tau}{(t-\tau)^\alpha}, \ 0 < \alpha < 1. \tag{1.5}$$

Concurrent with the development and improvement of pde-based models for image enhuncement, extensive efforts have been made to develop and introduce new computational approaches for dealing with image denoising techniques based on partial differential equations.
Here, an advanced computational approach based on meshless method will be formulated and used to solve the model (1.4) numerically. Meshless methods are an advanced class of techniques used in applied mathematics and scientific computing to numerically investigate and simulate the behavior of complicated practical models [13, 37]. The meshless methods are very powerful computational tools to deal with high-dimensional practical problems with complicated geometry domains. They are categorized into two main categories: 1- Those that are based on the strong forms of the governing model [4, 12, 30, 31, 36, 47, 48, 53, 55] and 2- Those that are based on the weak forms of the governing problem [16–19, 51, 52, 56]. To overcome some drawbacks of classical meshless methods, some straightforward approaches for the development of meshless methods based on thier localized formulation have been introduced. The local methods lead to a sparse and well-conditioned system of algebraic equations and are more stable than their global counterparts [5, 49, 50, 54, 58]. Recently, some meshless approaches have been used for dealing with pde-based image denoising [29, 32, 33].
In the current work, an efficient computational technique based on the combination of a semi-implicit time integration scheme and a localized meshless method in a domain decomposition framework would be performed to solve the time-fractional anisotropic difussion model (1.4).

## 2. Mathematical formulation

This section is devoted to formulate and implement a computational approach for solving the anisotropic sub-diffusion model (1.4). Firstly, a semi-implicit time discretization scheme is performed to discretize the model in the time direction. Then, a local meshless technique in the domain decomposition framework is formulated to fully discretize the model.

### 2.1. Time discretization.

In order to perform an efficient semi-implicit time integration scheme to discretize the governing equation (1.4) in the time direction, the time interval $[0,T]$ is divided into $L$ equal sub-intervals, $\bigcup_{k=0}^{L-1}[t_k,t_{k+1}]$ uniformly, where $t_k=k\Delta t$, $k=0,\cdots,L$ and $\Delta t=T/L$ ($\Delta t$ denotes the time step size). Using the backward Euler method, the Caputo time-fractional derivative at time level $t=t_{k+1}$ and for all $0\leq k\leq L-1$, can be approximated as follows:

$$\begin{aligned} {}_0^cD_t^{\alpha}u(\mathbf{x},t_{k+1}) &= \frac{1}{\Gamma(1-\alpha)}\int_0^{t_{k+1}}\frac{u_\tau(\mathbf{x},\tau)}{(t_{k+1}-\tau)^{\alpha}}d\tau \\ &= \frac{1}{\Gamma(1-\alpha)}\sum_{s=0}^{k}\frac{u(\mathbf{x},t_{s+1})-u(\mathbf{x},t_s)}{\Delta t}\int_{t_s}^{t_{s+1}}(t_{k+1}-\tau)^{-\alpha}d\tau+R_{k+1} \\ &= \frac{(\Delta t)^{-\alpha}}{\Gamma(2-\alpha)}\sum_{s=0}^{k}w_s(u^{k-s+1}-u^{k-s})+R_{k+1}, \end{aligned} \tag{2.1}$$

where $w_s=(s+1)^{1-\alpha}-s^{1-\alpha}$, $s=0,1,...,k$, $u^k=u(\mathbf{x},t_k)$ and $R_{k+1}$ denotes the truncation error of the discretization scheme, which satisfies for any $u(\mathbf{x},t)\in C^2(\Omega\times[0,\infty))$ in the following relation [57]:

$$\mid R_{k+1}\mid\leq\frac{1}{\Gamma(2-\alpha)}[\frac{1-\alpha}{12}+\frac{2^{2-\alpha}}{2-\alpha}-(1+2^{-\alpha})]\max_{0\leq t\leq t_{k+1}}|\frac{\partial^2u(\mathbf{x},t)}{\partial t^2}|(\Delta t)^{2-\alpha}.$$

Now, by rearranging (2.1), we obtain:

$${}_0^cD_t^{\alpha}u(\mathbf{x},t_{k+1})\approx\frac{(\Delta t)^{-\alpha}}{\Gamma(2-\alpha)}(u^{k+1}+\sum_{s=1}^{k}(w_{k-s+1}-w_{k-s})u^s-w_ku^0). \tag{2.2}$$

Substituting the approximation (2.2) for ${}_0^cD_t^\alpha u(\mathbf{x}, t_{k+1})$ into the governing fractional model (1.4), the following semi-implicit scheme at time level $t_{k+1}$ is obtained:

$$\frac{(\Delta t)^{-\alpha}}{\Gamma(2-\alpha)}(u^{k+1} + \sum_{s=1}^{k}(w_{k-s+1} - w_{k-s})u^s - w_k u^0) = \nabla \cdot (g(\mid \nabla G_\sigma * u^k \mid)\nabla u^{k+1}). \tag{2.3}$$

The semi-implicit discretization (2.3) treats $g(\mid \nabla G_\sigma * u^k \mid)$ explicitly, to avoid the nonlinearity of the diffusion coefficient that does not result in nonlinear algebraic problems. Moreover, the convolution term, $G_\sigma * u^k$ can be alternatively approximated by solving the homogeneous diffusion equation with the initial condition $u^k$. This linear equation can be solved numerically at the same domain by just one implicit step with length $\sigma$. In our implementation the convolution term in (2.3), is approximated by a function $u^\ell$, that is a solution of the diffusion equation discretized in the time direction by the backward Euler method with step $\sigma$, as follows [22]:

$$\frac{u^\ell - u^{k-1}}{\sigma} = \Delta u^\ell, \tag{2.4}$$

where $\Delta$ represents the 2D Laplace operator. Therefore, Equation (2.3) can be simplified as:

$$\frac{(\Delta t)^{-\alpha}}{\Gamma(2-\alpha)}(u^{k+1} + \sum_{s=1}^{k}(w_{k-s+1} - w_{k-s})u^s - w_k u^0) = \nabla \cdot (g(\mid \nabla u^\ell \mid)\nabla u^{k+1}). \tag{2.5}$$

The resulting equation at each time step can be rewritten as

$$\begin{aligned} \mathcal{L}u^{k+1} &= \mathcal{F}(u^k), \text{ in } \Omega, \\ \frac{\partial u^{k+1}}{\partial n} &= 0, \text{ on } \partial\Omega, \end{aligned} \tag{2.6}$$

wherein

$$\begin{aligned} \mathcal{L}u^{k+1} &= u^{k+1} - (\Delta t)^\alpha \Gamma(2-\alpha)\big[g(\mid \nabla u^\ell \mid)\Delta u^{k+1} + \frac{\partial g(\mid \nabla u^\ell \mid)}{\partial x}\frac{\partial u^{k+1}}{\partial x} + \frac{\partial g(\mid \nabla u^\ell \mid)}{\partial y}\frac{\partial u^{k+1}}{\partial y}\big], \\ \mathcal{F}(u^k) &= \sum_{s=1}^{k}(w_{k-s} - w_{k-s+1})u^s + w_k u^0. \end{aligned} \tag{2.7}$$

Now our interest is to study the time-independent problem (2.6).

2.2. **Spatial discretization.** In this section a localized version of RBF-based meshless method within a domain decomposition framework will be performed to study the time-independent equation (2.6).

2.2.1. *The overlapping domain decomposition method.* In PDE-based image processing and analysis, because of high computational cost required by numerical techniques, particularly for high-resolution images, some robust approaches have been proposed to reduce the complexity of the methods. Image-domain decomposition method is an efficient approach to reduce the complexity and computational cost associated with PDE-based image processing [14]. So in our implementation, a domain decomposition method is performed to reduce the computational costs of the large-scale image denoising problems. In this approach, the main computational domain, $\Omega$, is decomposed into several overlapping subdomains, $\Omega = \bigcup \Omega_i$, as depicted in Figure 1. Then, by considering the artificial boundaries, $\Gamma_i$, for each subdomain, the image denoising problem (2.6) can be implemented independently on each subdomain as follows:

$$\begin{aligned} \mathcal{L}u_i^{k+1} &= \mathcal{F}(u_i^k), \text{ in } \Omega_i, \\ \frac{\partial u_i^{k+1}}{\partial n} &= 0, \text{ on } \Gamma_i, \\ u^0 &= u_0(\mathbf{x}), \text{ in } \Omega_i. \end{aligned}$$

After reaching the desirable results by solving the image denoising problem on each subdomain, data exchange is done in order to match the inner pixels data. It is a good strategy that significantly reduces the computational cost per iteration and can be used for parallel processing purpose. In the next sub-section, two different numerical approaches

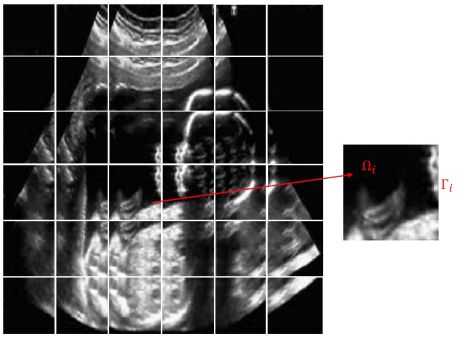


FIGURE 1. An image-domain decomposition scheme with overlapping subdomains, $\Omega_i$, and artificial boundaries, $\Gamma_i$.

are performed to fully discretize the proposed model.

2.2.2. *Explicit Finite Difference Approach.* As the first approach, the fractional model (1.4) is fully discretized by using an explicit finite difference method [64]

$$g^k_{i\pm1/2,j} = g\big(\big(\frac{u^k_{i\pm1,j}-u^k_{i,j}}{\Delta x}\big)^2\big), \quad g^k_{i,j\pm1/2} = g\big(\big(\frac{u^k_{i,j\pm1}-u^k_{i,j}}{\Delta y}\big)^2\big), \tag{2.8}$$

$$\begin{aligned} L^\alpha_t u^{k+1}_{i,j} &= \frac{1}{2(\Delta x)^2}\big(g^k_{i+1/2,j}(u^k_{i+1,j}-u^k_{i,j}) - g^k_{i-1/2,j}(u^k_{i,j}-u^k_{i-1,j})\\ &+\frac{1}{2(\Delta y)^2}\big(g^k_{i+1/2,j}(u^k_{i,j+1}-u^k_{i,j}) - g^k_{i,j-1/2}(u^k_{i,j}-u^k_{i,j-1}\big), \end{aligned}$$

where $L^\alpha_t u(x,t_{k+1}) \cong^c_0 D^\alpha_t u(x,t_{k+1})$ as given in (2.2).

2.2.3. *Localized RBF Meshless Method.* In this subsection, an efficient meshless computational procedure based on the localized RBF collocation approach is proposed to fully discretize the semi-discretized equation (2.6). In our approach, a set of regularly distributed field nodes, $\{x_j\}_{j=1}^N$, in each sub-domain is considered. For locally approximating, corresponding to each point, $x_j$, a local support domain, $\Omega_{x_j}$ contains $n(n \ll N)$ nearest neighbor points of $x_j$ is considered. So the function $u^k(x)$ is locally approximated as follows:

$$u^k(x) = \sum_{i=1}^{n} \lambda^k_i \phi_i(x), \quad x \in \Omega_{x_j}, \tag{2.9}$$

where $\phi_i(x) = \Phi(\|x-x_i\|)$ denotes a radial basis function centered at $x_i$, $\|x-x_i\|$ is the Euclidean distance between point of interest $x$ and center point $x_i$ and the coefficients $\{\lambda^k_i\}_{i=1}^n$ are unknown real constants should be determined. These unknown coefficients are determined by interpolating $u^k(x)$ at $n$ scattered nodes in the surrounding domain of $x$ as follows:

$$u^k(x_l) = \sum_{i=1}^{n} \lambda^k_i \phi_i(x_l), \quad l = 1,2,\ldots,n. \tag{2.10}$$

The linear system of algebraic equations (2.10) can be represented as follows:

$$\mathbf{U}^k = \mathbf{\Phi}\lambda^k, \tag{2.11}$$

where $\lambda^k = [\lambda^k_1, \lambda^k_2, ..., \lambda^k_n]^T$, and $\mathbf{\Phi}$ is the interpolation matrix:

$$\mathbf{\Phi} = \begin{bmatrix} \phi_1(x_1) & \phi_2(x_1) & \cdots & \phi_n(x_1) \\ \vdots & \vdots & \ddots & \vdots \\ \phi_1(x_n) & \phi_2(x_n) & \cdots & \phi_n(x_n) \end{bmatrix}. \tag{2.12}$$

It has been proved that for any set of $n$-distinct points and strictly positive definite RBFs, $\phi(x)$, the multivariate interpolation matrix, $\mathbf{\Phi}$, is non-singular [13]. So, the coefficient vector $\lambda^k$ can be calculated as follows:

$$\lambda^k = \mathbf{\Phi}^{-1}\mathbf{U}^k. \tag{2.13}$$

The value of function $u^k(x)$ at each interesting point $\bar{x} \in \Omega_{x_j}$ can be approximated as follows:

$$u^k(\bar{x}) = \mathbf{p^T}(\bar{x})\mathbf{\Phi}^{-1}\mathbf{U}^k = \mathbf{\Psi^T}(\bar{x})\mathbf{U}^k = \sum_{i=1}^{n} \Psi_i(\bar{x})u_i^k, \tag{2.14}$$

where $\mathbf{p}(\bar{x}) = [\phi_1(\bar{x}), \phi_2(\bar{x}), ..., \phi_n(\bar{x})]^T$, $\mathbf{\Psi}(\bar{x}) = \mathbf{p^T}(\bar{x})\mathbf{\Phi}^{-1} = [\Psi_1, \Psi_2, ..., \Psi_n]^T$. The data dependent shape functions, $\Psi_i$, $i = 1, ..., n$ are compactly supported shape functions. The partial derivatives of first and higher orders of shape function $\Psi$ are obtained as follows:

$$\frac{\partial \mathbf{\Psi}}{\partial x} = [\frac{\partial \Psi_1}{\partial x}, \frac{\partial \Psi_2}{\partial x}, ..., \frac{\partial \Psi_n}{\partial x}]^T = \frac{\partial \mathbf{P^T}(x)}{\partial x}(\Phi)^{-1}, \tag{2.15}$$

where

$$\frac{\partial \mathbf{P}}{\partial x} = [\frac{\partial \phi_1}{\partial x}, \frac{\partial \phi_2}{\partial x}, ..., \frac{\partial \phi_n}{\partial x}]^T. \tag{2.16}$$

Also,

$$\frac{\partial^m \mathbf{\Psi}}{\partial x^m} = \frac{\partial^m \mathbf{P^T}(x)}{\partial x^m}(\Phi)^{-1}. \tag{2.17}$$

Therefore, we have:

$$\frac{\partial^m u^k(x)}{\partial x^m} = \Big(\frac{\partial^m \mathbf{\Psi}}{\partial x^m}\Big)^T \mathbf{U}^k. \tag{2.18}$$

Derivative with respect to y (first derivatives or higher) can be calculated in the same way. Substituting the representation (2.10) into the relations (2.7) and collocating these equations at collocation points $\{x_j\}_{j=1}^n$, we have:

$$\begin{aligned}
&\sum_{i=1}^{n} \Psi_i(x_j)u_i^{k+1} - (\Delta t)^\alpha \Gamma(2-\alpha)\Big(g(\mid \nabla u^\ell \mid)\sum_{i=1}^{n} \Delta\Psi_i(x_j)u_i^{k+1} + \frac{\partial g(\mid \nabla u^\ell \mid)}{\partial x}\sum_{i=1}^{n}\frac{\partial \Psi_i(x_j)}{\partial x}u_i^{k+1} \\
&+\frac{\partial g(\mid \nabla u^\ell \mid)}{\partial y}\sum_{i=1}^{n}\frac{\partial \Psi_i(x_j)}{\partial y}u_i^{k+1}\Big) \\
&= \omega_k \sum_{i=1}^{n} \Psi_i(x_j)u_i^0 + \sum_{s=1}^{k}\sum_{i=1}^{n}[(\omega_{k-s} - \omega_{k-s+1})\Psi_i(x_j)u_i^s], \quad x_j \in \Omega_m, \\
&\text{and} \\
&\sum_{i=1}^{n}\frac{\partial \Psi_i(x_j)}{\partial n}u_i^{k+1} = 0, \quad x_j \in \partial\Omega_m.
\end{aligned} \tag{2.19}$$

For each subdomain, the above relations lead to a linear system of algebraic equations with a well-conditioned and sparse coefficient matrix. The process will be repeated for each time level until a desirable result is achieved.

## 3. Numerical results

This section is devoted to investigate the performance of the proposed mathematical model and formulated computational procedure for reducing the speckle noise from the medical ultrasound image. In order to illustrate the effectiveness of the proposed methods, a real ultrasound image (240 × 240 pixels) (see Fig. (2-a)) which has been

corrupted by speckle noise with variance of 0.12 (see Fig. (2-b)), is considered. To test the proposed algorithms and assess their performance, we use the signal-to-noise ratio (SNR):

$$SNR = 10 \cdot \log_{10} \frac{\sigma^2_{u^\star}}{\sigma^2_{u^k - u^\star}}, \tag{3.1}$$

where $u^\star$ denotes the uncorrupted image and $\sigma^2$ is the variance corresponds to the signals. The proposed computational techniques have been performed to deal with the corrupted medical image. Firstly, the formulated explicit finite difference approach, Eq (2.8), is used to enhance the quality of image. The result is presented as Fig. (2-c). This result is obtained by considering $\Delta t = 0.01$, $k = 1/2$, $\alpha = 0.38$ and after 30 iterations. Also, the proposed localized RBF collocation method is used for noise reduction of the image. In our implementation, to reduce the computational cost of the method, the suggested domain decomposition strategy is used to divide the image into thirty six overlapping subdomains with the same number of pixels (see Fig 1). Also, to reduce the influence of boundary conditions on the inner pixels near the artificial boundaries, some segments with overlapping of width 10 pixels are considered. Moreover, the Gaussian radial basis function, $\phi(x) = e^{-\epsilon^2 \|x\|^2}$ is used as the shape function. Fig (2-d) illustrates the result obtained by using the approach. This result is obtained by choosing $\sigma = 0.0001$, $\Delta t = 0.01$, $n = 9$ (stencil points), $k = 1/2$, $\alpha = 0.59$ and after 30 iterations. Also, the results are compared with the result obtained by using the classical Catté's pde model (1.2 ) and speckle reducing anisotropic diffusion filter [66], as shown in Fig (2-e) and Fig (2-f), respectively.

In order to investigate the effect of fractional-order, $\alpha$, on the efficiency of the fractional diffusion model and accuracy of the results, SNR values versus the values of fractional-order, $\alpha$, are illustrated in the figures 3 and 4. The results demonstrate that the optimal values of fractional-order for the proposed explicit finite difference approach and localized RBF collocation method are $\alpha = 0.38$ and $\alpha = 0.59$, respectively. Finally, the SNR values of results computed from the proposed approaches for some values of fractional-order and two types of noisy images are presented and compared with the classical Catté's pde model and speckle reducing anisotropic diffusion filter [66], in Table (1). The results confirm the efficiency of the proposed fractional model compared to the classical Catté's model.

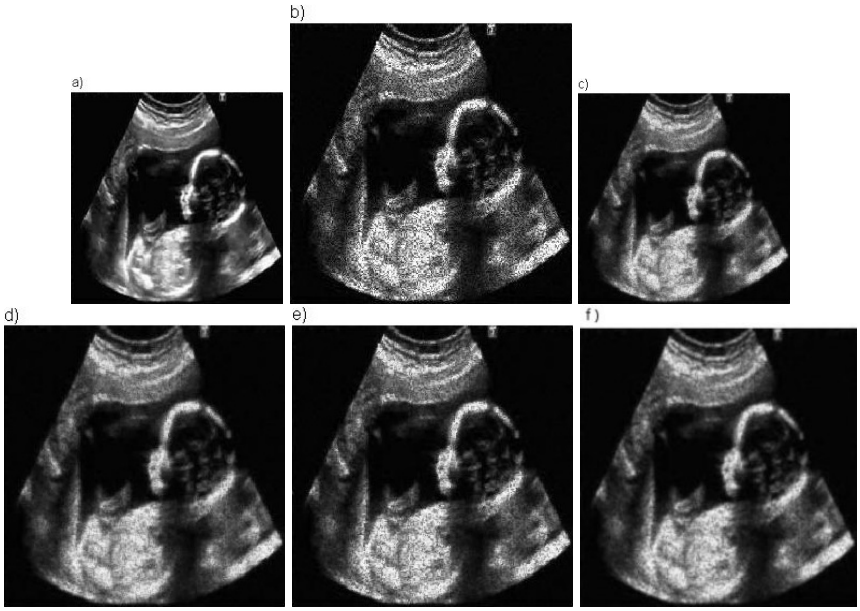


FIGURE 2. Numerical results of the restoration a noisy image with 30 iterations. (a) Original image. (b) noisy image. (c) Results of the method-1 with $\alpha = 0.38$ (d) Results of the method-2 with $\alpha = 0.59$ (e) Result of Catté's model (f) Result of the speckle reducing anisotropic diffusion filter [66].

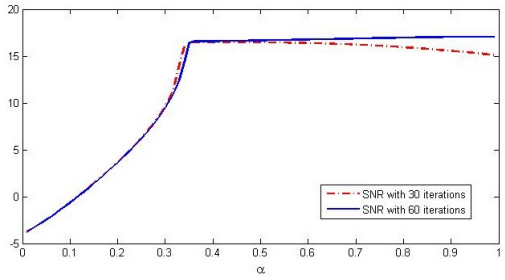


FIGURE 3. SNR values as function of $\alpha$ for method 1.

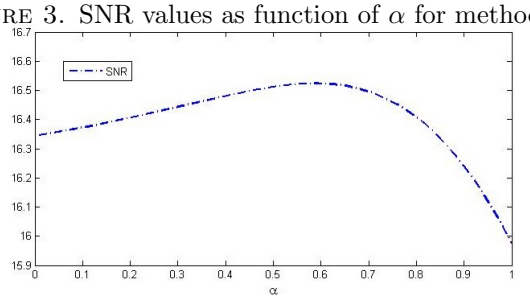


FIGURE 4. SNR values as function of $\alpha$ for method 2.

TABLE 1. SNR obtained for different values of $\alpha$ with 30 iterations.

| *Speckle noise* | $\alpha$ | 0.38 | 0.59 | 0.8 | 1(Catté's model) |
|---|---|---|---|---|---|
| $variance = 0.12$ | Method 1 | 16.4849 | 16.3893 | 15.9356 | 15.0606 |
| | Method 2 | 16.4738 | 16.5235 | 16.4083 | 15.9765 |
| | [66] | | | | 16.2031 |
| $variance = 0.20$ | Method 1 | 14.3311 | 14.2113 | 14.1551 | 13.8021 |
| | Method 2 | 14.3092 | 14.4928 | 14.2112 | 13.9823 |
| | [66] | | | | 14.1805 |

## 4. CONCLUSIONS

The primary purpose of this study was to improve a nonlinear anisotropic diffusion filter for ultrasound image speckle reduction in both modelling and solution approaches. In terms of modelling, an interesting, time-fractional anisotropic diffusion filter based on fractional calculus theory has been proposed. The suggested time-fractional anisotropic diffusion model is used to reduce the speckle noise and enhance the quality of the medical ultrasound image. The diffusion process is controlled by adaptively setting the fractional-order, $\alpha$. In terms of numerical procedure, two efficient computational schemes are formulated and used to solve the fractional model. Especially, an interesting and powerful localized meshless technique within a domain decomposition framework is performed to solve the problem. The proposed approach significantly reduce the computational cost and leads to a well-conditioned and sparse linear system of algebraic equations. The performance of the proposed de-speckling procedure was examined on ultrasound image. The de-speckling results obtained with the proposed fractional model were compared with the classical Catté's model. From the numerical results, we can conclude that the proposed approach is superior to the classical Catté's model. Besides, the fractional calculus theory can be used to extend and propose a more general time-space fractional Catté's model. Moreover, the localized meshless method in the domain decomposition framework can be implemented on parallel multiprocessor machines, which is promising in developing approaches for large-scale pde-based image processing.

## Acknowledgment

The authors would like to express their thankfulness to anonymous referees for their helpful constructive comments.

## References

[1] R. Abazari and M. Lakestani, *Fourier based discrete shearlet transform for speckle noise reduction in medical ultrasound images*, Current Medical Imaging Reviews., *14* (2018), 447–483.
[2] R. Abazari and M. Lakestani, *A hybrid denoising algorithm based on shearlet transform method and yaroslavskys filter*, Multimedia Tools and Applications., *77* (2018), 17829–17851.
[3] R. Abazari and M. Lakestani, *Non-subsampled shearlet transform and log-transform methods for despeckling of medical ultrasound images*, Informatica., *30* (2019), 1–19.
[4] S. Abbasbandy, H. R. Ghehsareh, and I. Hashim, *A meshfree method for the solution of two-dimensional cubic nonlinear Schrödinger equation*, Engineering Analysis with Boundary Elements., *37* (2013), 885–898.
[5] S. Abbasbandy, H. R. Ghehsareh, I. Hashim and A. Alsaedi, *A comparison study of meshfree techniques for solving the two-dimensional linear hyperbolic telegraph equation*, Engineering Analysis with Boundary Elements., *40* (2014), 10–20.
[6] L. Alvarez, P.-L. Lions, and J.-M. Morel, *Image selective smoothing and edge detection by nonlinear diffusion*, SIAM Journal on numerical analysis., *29* (1992), 845–866.
[7] G. Aubert and P. Kornprobst, *Mathematical problems in image processing: partial differential equations and the calculus of variations*, volume 147. Springer Science & Business Media, 2006.
[8] J. Bai and X.-C. Feng, *Fractional-order anisotropic diffusion for image denoising*, IEEE transactions on image processing., *16*(2007), 2492–2502.
[9] F. Catté, P.-L. Lions, J.-M. Morel, and T. Coll, *Image selective smoothing and edge detection by nonlinear diffusion*, SIAM Journal on Numerical analysis., *29*(1992), 182–193.
[10] R. N. Czerwinski, D. L. Jones, and W. D. O'brien, *Line and boundary detection in speckle images*, IEEE Transactions on Image Processing., *7*(1998), 1700–1714.
[11] S. Das and I. Pan, *Fractional order signal processing: introductory concepts and applications*, Springer Science & Business Media, 2011.
[12] M. H. Esfahani, H. R. Ghehsareh, and S. K. Etesami, *The extended method of approximate particular solutions to simulate two-dimensional electromagnetic scattering from arbitrary shaped anisotropic objects*, Engineering Analysis with Boundary Elements., *82* (2017), 91–97.
[13] G. E. Fasshauer, *Meshfree approximation methods with MATLAB*, volume 6, World Scientific, 2007.
[14] D. Firsov and S. Lui, *Domain decomposition methods in image denoising using gaussian curvature*, Journal of Computational and Applied Mathematics., *193* (2006), 460–473.
[15] H. R. Ghehsareh, A. Majlesi, and A. Zaghian, *Lie symmetry analysis and conservation laws for time fractional coupled whitham-broer-kaup equations*, UPB Sci. Bull. Ser. A Appl. Math. Phys., *80* (2018), 153–168.
[16] H. R. Ghehsareh, M. Raei, and A. Zaghian, *Application of meshless local petrov- galerkin technique to simulate two-dimensional time-fractional tricomi-type problem*, Journal of the Brazilian Society of Mechanical Sciences and Engineering., *41* (2019), 252.
[17] H. R. Ghehsareh, M. Raei, and A. Zaghian, *Numerical simulation of a modified anomalous diffusion process with nonlinear source term by a local weak form meshless method*, Engineering Analysis with Boundary Elements., *98* (2019), 64–76.
[18] H. R. Ghehsareh, A. Zaghian, and M. Raei, *A local weak form meshless method to simulate a variable order time-fractional mobile-immobile transport model*, Engineering Analysis with Boundary Elements., *90* (2018), 63–75.
[19] H. R. Ghehsareh, A. Zaghian, and S. M. Zabetzadeh, *The use of local radial point interpolation method for solving two-dimensional linear fractional cable equation*, Neural Computing and Applications., *29* (2018), 745–754.
[20] J. W. Goodman, *Some fundamental properties of speckle*, JOSA., *66* (1976), 1145–1150.
[21] F. Guan, P. Ton, S. Ge, and L. Zhao, *Anisotropic diffusion fltering for ultrasound speckle reduction*, Science China Technological Sciences., *57* (2014), 607–614.

[22] A. Handlovičová, K. Mikula, and F. Sgallari, *Variational numerical methods for solving nonlinear diffusion equations arising in image processing*, Journal of Visual Communication and Image Representation., *13* (2002), 217–237.
[23] X. Hao, S. Gao, and X. Gao, *A novel multiscale nonlinear thresholding method for ultrasonic speckle suppressing*, IEEE Transactions on Medical Imaging., *18* (1999), 787–794.
[24] M. Hashemi and A. Akgül, *Solitary wave solutions of time-space nonlinear fractional schrodingers equation: two analytical approaches*, Journal of Computational and Applied Mathematics., *339* (2018), 147–160.
[25] M. Hashemi and Z. Balmeh, *On invariant analysis and conservation laws of the time fractional variant boussinesq and coupled boussinesq-burgers equations*, The European Physical Journal Plus., *133* (2018), 427.
[26] M. Hashemi, M. Inc, M. Parto-Haghighi, and M. Bayram, *On numerical solution of the time-fractional diffusion-wave equation with the fictitious time integration method*, The European Physical Journal Plus., *134* (2019), 488.
[27] K. Höllig and J. A. Nohel, *A diffusion equation with a nonmonotone constitutive function*, Systems of Nonlinear Partial Differential Equations., Springer. (1983), 409–422.
[28] M. Janev, S. Pilipović, T. Atanacković, R. Obradović, and N. Ralević, *Fully fractional anisotropic diffusion for image denoising*, Mathematical and Computer Modelling., *54* (2011), 729–741.
[29] M. Kamranian, M. Dehghan, and M. Tatari, *An image denoising approach based on a meshfree method and the domain decomposition technique*, Engineering Analysis with Boundary Elements., *39* (2014), 101–110.
[30] E. J. Kansa, *Multiquadricsa scattered data approximation scheme with applications to computational fluid-dynamicsi surface approximations and partial derivative estimates*, Computers & Mathematics with applications., *19* (1990), 127–145.
[31] M. Khaksarfard, Y. Ordokhani, M. S. Hashemi, and K. Karimi, *Space-time radial basis function collocation method for one-dimensional advection-diffusion problem*, Computational Methods for Differential Equations., *6* (2018), 426–437.
[32] M. A. Khan, W. Chen, Z. Fu, and A. Ullah, *Meshfree digital total variation based algorithm for multiplicative noise removal.*, J. Inf. Sci. Eng., *34* (2018), 1441–1468.
[33] M. A. Khan, W. Chen, A. Ullah, and Z. Fu, *A mesh-free algorithm for rof model.*, EURASIP Journal on Advances in Signal Processing., *53* (2017) .
[34] S. Kichenassamy, *The perona-malik paradox.*, SIAM Journal on Applied Mathematics., *57* (1997), 1328–1342.
[35] J.-S. Lee, *Digital image enhancement and noise filtering by use of local statistics.*, IEEE Transactions on Pattern Analysis & Machine Intelligence., *2* (1980), 165–168.
[36] L. Ling, R. Opfer, and R. Schaback, *Results on meshless collocation techniques.*,Engineering Analysis with Boundary Elements., *30* (2006), 247–253.
[37] G.-R. Liu and Y.-T. Gu, *An introduction to meshfree methods and their programming.*,Springer Science & Business Media, 2005.
[38] C. P. Loizou and C. S. Pattichis, *Despeckle filtering algorithms and software for ultrasound imaging.*, Synthesis lectures on algorithms and software in engineering., *1* (2008), 166.
[39] A. Majlesi, H. R. Ghehsareh, and A. Zaghian, *On the fractional jaulent-miodek equation associated with energy-dependent schrodinger potential: Lie symmetry reductions, explicit exact solutions and conservation laws.*, The European Physical Journal Plus., *132* (2017), 516.
[40] J. L. Mateo and A. Fernández-Caballero, *Finding out general tendencies in speckle noise reduction in ultrasound images.*, Expert systems with applications., *36* (2009), 7786–7797.
[41] N. Mohamadi, A. R. Soheili, and F. Toutounian, *A denoising pde model based on isotropic diffusion and total variation models.*, Computational Methods for Differential Equations., *8* (2020), 815–826.
[42] P. Noras and N. Aghazadeh, *New denoising and edge detection scheme based on rationalized haar functions.*, MACHINE VISION AND IMAGE PROCESSING., *5* (2018), 99–111.
[43] P. Perona and J. Malik, *Scale-space and edge detection using anisotropic diffusion.*, IEEE Transactions on pattern analysis and machine intelligence., *12* (1990), 629–639.

[44] P. Perona, T. Shiota, and J. Malik, *Anisotropic diffusion.*, In Geometry-driven diffusion in computer vision., Springer, (1994), 73–92.
[45] Y. Povstenko, *Fractional thermoelasticity.*, In Geometry-driven diffusion in computer vision., volume 219. Springer, 2015.
[46] E. Ritenour, T. Nelson, and U. Raff, *Applications of the median filter to digital radiographic images.*, In ICASSP'84. IEEE International Conference on Acoustics, Speech, and Signal Processing., volume 9 (1984), 251–254.
[47] H. Roohani Ghehsareh, M. Hajisadeghi Esfahani, and S. Kamal Etesami, *Numerical simulation of electromagnetic wave scattering from perfectly conducting cylinders using the local radial point interpolation technique.*, Journal of Electromagnetic Waves and Applications., *33* (2019), 335–349.
[48] H. Roohani Ghehsareh, M. S. Seidzadeh, and S. K. Etesami, *Numerical simulation of a generalized anomalous electro-diffusion process in nerve cells by a localized meshless approach in pseudospectral mode.*, International Journal of Numerical Modelling: Electronic Networks, Devices and Fields., (2020).
[49] M. Safarpoor and A. Shirzadi, *Numerical investigation based on radial basis function- finite-difference (rbf-fd) method for solving the stokes-darcy equations.*, Engineering with Computers., (2019).
[50] M. Safarpoor, F. Takhtabnoos, and A. Shirzadi, *A localized rbf-mlpg method and its application to elliptic pdes.*, Engineering with Computers., (2019).
[51] A. Shirzadi, *Solving 2d reaction-diffusion equations with nonlocal boundary conditions by the rbf-mlpg method.*, Computational Mathematics and Modeling., *25* (2014), 521–529.
[52] A. Shirzadi, L. Ling, and S. Abbasbandy, *Meshless simulations of the two-dimensional fractional-time convection-diffusion-reaction equations.*, Engineering analysis with boundary elements., *36* (2012), 1522–1527.
[53] E. Shivanian, *Pseudospectral meshless radial point hermit interpolation versus pseudospectral meshless radial point interpolation.*, International Journal of Computational Methods., (2019).
[54] E. Shivanian and H. Fatahi, *Analysis of meshless local radial point interpolant on a model in population dynamics.*, Computational Methods for Differential Equations., *7* (2019), 276–288.
[55] E. Shivanian and A. Jafarabadi, *Two-dimensional capillary formation model in tumor angiogenesis problem through spectral meshless radial point interpolation.*, Engineering with Computers., (2019).
[56] V. Sladek, J. Sladek, and A. Shirzadi, *The local integral equation method for pattern formation simulations in reaction-diffusion systems.*, Engineering Analysis with Boundary Elements., *50* (2015), 329–340.
[57] Z.-z. Sun and X. Wu, *A fully discrete difference scheme for a diffusion-wave system.*, Applied Numerical Mathematics., *56* (2006), 193–209.
[58] F. Takhtabnoos and A. Shirzadi, *A local meshless method based on the nite collocation and local integral equations method for delay pdes.*, Engineering Analysis with Boundary Elements., *83* (2017), 67–73.
[59] V. V. Uchaikin, *Fractional derivatives for physicists and engineers.*, volume 2. Springer, 2013.
[60] L. A. Vese and S. J. Osher., *Modeling textures with total variation minimization and oscillating patterns in image processing.*, Journal of scientific computing., *19* (2003), 553–572.
[61] R. F. Wagner., *Statistics of speckle in ultrasound B-scans.*, IEEE Trans. Sonics & Ultrason., *30* (1983), 156–163.
[62] J. Weickert., *Anisotropic diffusion in image processing.*, volume 1. Teubner Stuttgart, 1998.
[63] J. Weickert and C. Schnörr, *Pde-based preprocessing of medical images.*, 2000.
[64] M. Wielgus., *Perona-malik equation and its numerical properties.*, arXiv preprint arXiv:1412.6291, 2014.
[65] Q. Yang, D. Chen, T. Zhao, and Y. Chen, *Fractional calculus in image processing: a review.*, Fractional Calculus and Applied Analysis., *19* (2016), 1222–1249.
[66] Y. Yu and S. T. Acton, *Speckle reducing anisotropic diffusion.*, IEEE Transactions on image processing., *11* (2002), 1260–1270.
[67] J. Zhang and Z. Wei, *Fractional variational model and algorithm for image denoising.*, In 2008 Fourth International Conference on Natural Computation., volume 5, pages 524-528. IEEE, 2008.
[68] J. Zhang, Z. Wei, and L. Xiao, *Adaptive fractional-order multi-scale method for image denoising.*, Journal of Mathematical Imaging and Vision., *43* (2012), 39–49.